SkyIsland: Aerial Docking Drone System

ECE 4012 Senior Design Project

SKYISLAND

Advisor: Dr. Jennifer Hasler

Latifah Almaghrabi, lalmaghrabgi3@gatech.edu
Adrian de la Iglesia Valls, aliv3@gatech.edu
Ayca Ermis, aycaermis@gatech.edu
Jiaqing Li, jli651@gatech.edu
Lingfeng Zhou, lingfeng_zhou@gatech.edu

Submitted

May 3rd, 2018

Table of Contents

Executive Summary

SkyIsland is a drone system comprised of independent quadrotors with the ability to interlock and reconfigure into one collective drone structure. The reconfigured drone structure has the ability to reverse the formation by breaking apart into its constituent drones. The system can reassemble itself based on the characteristics of the assigned task and the required features to execute it.

The flexibility of the system makes it versatile and adaptable in applications involving search and rescue in hazardous areas, cargo delivery, military recon, and difficult inspections in inaccessible regions. The ability for the drones to reconfigure and reshape provides flexibility in unnavigable regions, such as narrow canyons and dense forests while minimizing air traffic in open and congested areas.

When reassembling into a collective structure, electro-permanent magnets were utilized as a holding force to maintain the connection between coupled drones. Rangefinders and optical detectors were employed to achieve mid-air alignment between approaching drones in preparation for docking. The system uses complex control systems to guide constituent drones when docking mid-air. Drone interactions will be integrated into a centralized software platform coupled to a human machine interface at a central ground station.

Several open-source and proprietary software toolsets were available for the implementation of the SkyIsland system which kept development costs reasonable. The project is currently estimated to cost $2000.00 which will fund both the material costs of prototyping, associated labor, as well as acquiring any relevant software licensing.

SkyIsland: Aerial Docking Drone System

1. Introduction

The SkyIsland team designed and prototyped a search and inspection drone system featuring mid-air self-docking and undocking prompted from commands sent through the ground control station. The team expended $1000.00 thus far to develop a prototype set for SkyIsland and expects to spend another $1000.00 for the project's continuation.

1.1 Objective

The team designed and prototyped a system of two drones that was intended to perform stabilized self-docking and undocking mid-air to achieve dynamic, in-mission reconfiguration, high payload capacity, and multifunctionality. Inputs from the operator include movement directions (i.e. forward, backward, left and right) as well as docking and undocking commands. Individual drones operate independently until a docking command is received. When the docking command is received, the two prototype drones can aggregate together, perform mid-air docking, and operate in unity to perform a joint task. When an undocking command is received, the two drones will separate, and will be ready to perform individual tasks.

1.2 Motivation

Most commercially available drones operate individually limited to a singular functionality. There is no available solution in the drone market which utilizes a drone system with mid-air docking and undocking. Mid-air docking and reconfiguration of drones is a relatively unexplored topic in the research area as well. One comparable project in research is Daniel Wilson's unmanned aerial vehicles with airborne docking, from the University of Sydney. However, this research only concerns mid-air refueling of human-sized aircrafts. This investigated solution also requires specific shapes of the leader and follower drones, namely a cone-shaped, parachute-like drogue and nose [1].

The motivation behind the SkyIsland system is to introduce a multipurpose and easy-to-assemble inspection drone system into the developing drone market. The team aspires to design a prototype that, when manufactured in large scale, will be cost-effective and possesses a wide variety of applications. The primary customer base for SkyIsland comprises of communications, power, search & rescue, and defense companies and organizations.

1.3 Background

The closest commercial product to SkyIsland is the on-ground self-recharging inspection drone DRONEBOX from H3 Dynamics [1]. Mid-air docking, however, as previously mentioned has been explored as a research topic for mid-air refueling of human-sized aircrafts [2]. Four key components are paramount to SkyIsland's prototype design: drone docking/locking coupling, drone localisation, stability control, and software integration. An abundance of research is already conducted in these distinct areas. Using electro-permanent magnet as a locking mechanism has been employed in M-blocks, a product developed by researchers at MIT. By activating and deactivating electro-permanent magnets in certain patterns, cubes interlock and reconfigure into a collective structure [3]. Additionally, the interlocking of robotic modules employs position sensors to bring modules into proximity of each other, before activating electro-permanent magnets. Won et al. shows, signal strength is mathematically related to distance and angle between emitter and receiver of a pair of position sensors [4]. At a fixed distance, robotic modules can be aligned based on signal strength. For stability control, the Euler-Newton equation applies to all models regardless of their geometries or number of rotors. The mathematical model is a set of equations that can determine the response of the motors to given reference commands and disturbances [5].

2. Project Description and Goals

The main goal of this project is to design a drone system enabled with a docking mechanism that allows two or more drones to dock in mid-flight and operate as one unit. Docking will be achieved using switchable electro-permanent magnets. The magnetic interlock mechanism will be designed by the team and installed on an outer shell onto the drones comprising the system. The design of the interlock mechanism will include an isolated power source from the drone's main power source. The drone system will be comprised of a complex control system to manage flight stability, path planning and flight execution. The final product would be excellent for search and inspection applications. The ability to dock more than two drones together allows the system to maximize efficiency in rotor operation for a larger drone structure. This modularity allows the optimal utilization of current resources to diversify the capabilities of user. It also offers much more flexibility and optimization. Assuming that the design is adaptable to any drone, the target price for a kit of two drones is $1600.

The final output for the project will feature the following:

- The ability to fly with great stability to accomplish an assigned task in three different modes:
    - Autonomously
        - Each of the drones comprising the system can fly as one individual unit
    - As one docked unit
        - Magnetic interlock is activated, the drones in the system are docked together and
    - operate as a single unit
    - As a swarm
        - The drones comprising the system are on standby for a docking command from ground. They are not physically attached, but their behavior and flight control is influenced by the other drones in the swarm

- Mid-flight autonomous alignment and docking
    - Each of the drones comprising the system has active and passive sites on its outer shell. An active site on a drone locks with a passive site on another drone. These sites are defined as the following
        - Active Sites: locations where a controllable electro-permanent magnet is installed
        - Passive Sites: locations where a soft magnetic material is installed
    - Magnetic interlock maintains its holding force without actively consuming power during docked flight
    - Alignment is achieved by the utilization of the ultrasonic sensors, optical sensors and GPS
- Wireless communication and Network
    - The drones comprising the system are connected to a local area wireless network
    - Drone-to-drone communication is utilized significantly during alignment before docking
    - Drone-to-ground communication is maintained at all times

3. Technical Specifications & Verification

TABLE 3
HARDWARE TECHNICAL SPECIFICATION

Hardware Feature	**Proposed Specification**	**Updated Specification**
Position Sensor Detection Range	> 10 m	5 m
Alignment Sensor Sensitivity	< 1 cm	5 mm
Minimum Re-polarization Magnetic Field	> 50 kA/m	>153 kA/m
Drone-to-Drone Communication Control Distance	> 20 m	100 m
Drone-to-Ground Communication Control Distance	~100 m	1000 m
Regulated Power Supply	< 5 V	4.7 V
Flight Duration	> 5 minutes	8 min

TABLE 4
SIMULATED TECHNICAL SPECIFICATIONS

Simulated Features	**Original Specification**	**Updated Specification**
Amount of Command Input	< 12 inputs	8 inputs
Bit Rate	125 kbs/s	To be implemented
Communication Latency	< 250 ms	To be implemented
Orientation precision	±5º	±1.15º at worst tested case
Position Precision	±5 cm	±8.1 cm at worst tested case
Stability Correction Rate	> 100 Hz	100 Hz

4. Design Approach and Details

4.1 Design Approach

4.1.1 Microcontroller Choice

Software integration is a key component to the SkyIsland system. In an attempt to strike a fine balance between small hardware packaging, minimized power consumption, and functionality, the Beaglebone Blue (BB Blue) microcontroller was chosen as the microcontroller solution with the intention of governing both the docking electronics and the basic flight routines on a SkyIsland drone unit. The BB Blue microcontroller comes equipped with an IMU/Barometer, specialized connectors for drone electronic speed control (ESC) units, and WiFi/Bluetooth capability. The BB Blue microcontroller is powered by an 1GHz ARM-Cortex A8 processor situated on an Octavo Systems OSD3358 "system on a chip" (SoC).

In addition to its IMU/Barometer, ESC unit control, and wireless capabilities, the BB Blue microcontroller supports digital and analog general purpose I/O (GPIO) capabilities similar to those found on the Arduino Nano microcontroller used for prototyping SkyIsland's electro-permanent magnet circuitry as well as the time-of-flight drone orientation system. As a result, the BB Blue allows for the separate software implementations and hardware prototypes of SkyIsland components to be unified under a single computing apparatus, tied together through the BB Blue's GPIO, built-in IMU, and desktop-grade Debian OS. However, the lack of available codebase for the BB Blue platform made software development very difficult. At first, the lack of support and development on the open-source ArduPilot software platform for Beaglebone hardware prevented the implementation of an on-board pre-baked flight solution. Then, the Robot Operating System (ROS) was considered as the software solution for the project. The latest version of ROS, however, does not support the latest BB Blue Debian 9 OS image, and running an outdated OS on the BB Blue introduced driver-level limitations to the BB Blue which is a relatively new and in-development product which are outside the scope of the project to resolve, so an outdated implementation of the Robot Operating System (ROS) was built from the source on a supported version of the Debian 8.7 image on the BB Blue. Unfortunately, the compiled ROS software distribution offered limited tool sets for outdoor drone flight and developing basic flight control software from scratch using the ROS API is outside the scope of the project. After all these considerations in software development and choice, a MATLAB & Simulink software solution was ultimately chosen as code blocks and drivers were more readily available for Beaglebone hardware through the Simulink Embedded Coder software suite. Therefore, due to the lack of available codebase for the BB Blue platform, an alternative but similar platform with a more comprehensive codebase both from open-source software distributions and MathWorks, Beaglebone Black (BB Black), will be used in-place of the BB Blue during prototyping and final software integration will be ported back to the BB Blue.

4.1.2 Positioning Sensors

This project utilized VL53L0X and VL6180X time-of-flight sensors for close-range relative positioning and drone alignment. Both sensors employs LIDAR technology to detect distance.

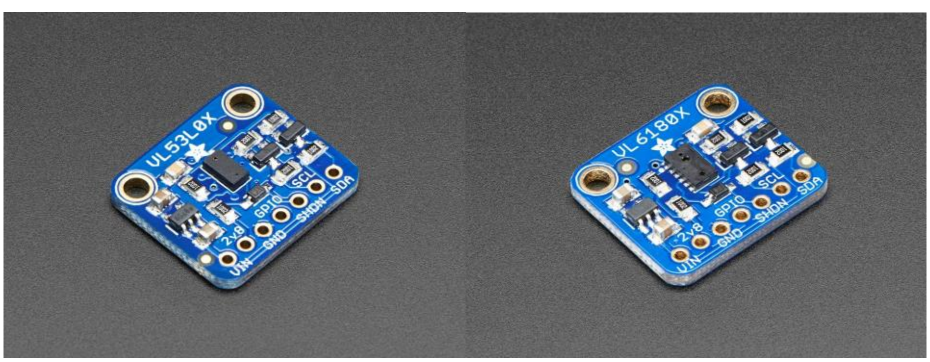

Figure 1. Sensor modules used in SkyIsland. (a) VL53L0X ToF sensor [6] (b) VL6180X ToF sensor [7]

VL53L0X time-of-flight (ToF) distance sensor was chosen to be implemented on the bottom of each drone to determine drones' altitude since the BeagleBone Black microcontroller does not have an integrated IMU. VL53L0X sensor contains a laser source and a matching sensor to determine the proximity of the object based on how long it takes for laser to bounce back on the object. VL53L0X is ideal for altitude measurement since its detection range is from 50 to 1200mm which is enough altitude to demonstrate mid-flight docking [6].

For close-range positioning and alignments of drones, VL6180X time-of-flight sensors were considered. VL6180X sensors operate on the same logic as VL53L0X and provide distance measurements from 5 to 100mm. the upper limit of the operating range could go up to 150-200mm with good ambient conditions [7]. For this project, a short range alignment sensor system was built using two VL6180X sensors mounted at the same level 63.5mm apart from each other. The short range alignment system is to be mounted on each active side on the drone shell. For prototyping, an Arduino was used to test the operation of alignment. Running the system on Arduino, the difference between the distances measured by each of the VL6180X sensors was taken in to calculate the orientation of one drone relative to one another. The logic for these calculations is as shown in Figure 2.

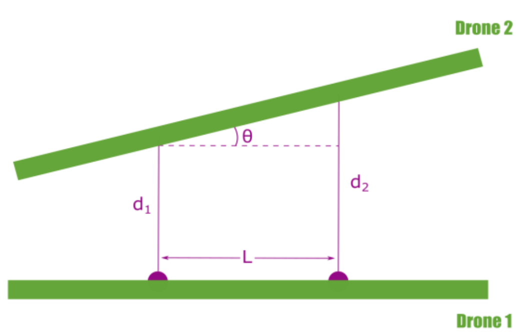

$$L = 63.5$$

$$\tan(\theta) = \frac{|d_1 - d_2|}{L}$$

$$\theta = atan2(|d_1 - d_2|, L) * \frac{180°}{\pi}$$

Figure 2. Diagram representation and mathematical equations outlining relative drone orientations.

In the Arduino program for the VL6180X sensors, whenever the orientation of Drone 2 is less than 10° ($\theta < 10°$) and distances d1 and d2 are less than 50mm ($d_1 < 50$and $d_2 < 50$), a signal was transmitted from the Arduino with two VL6180X sensors to a receiving Arduino via an nRF24L01 transceiver to mimic the envisioned communication between ToF sensors and magnet mechanism. Communication between the receiver Arduino and the transmitter Arduino with the alignment sensor system verified by blinking an LED on the receiver end when the signal is received. In future implementations of the project, the alignment system will be implemented on the BeagleBone board via Simulink code blocks and they will be utilized to initiate the polarization of the magnets and thus the docking process.

4.1.3 Vision for Localization

A camera was employed for long and midrange relative positionings of the drones. Long range drone tracking was performed with the Kalman filter, and midrange distance and orientation estimation were achieved with the ArUco marker.

The Kalman filter detects moving object in the frame. The first 30 frames of a video were used for background training. The motion parameter was specified as constant velocity. The minimum movement object size was picked to be 100 pixels, which means a moving object in the frame has to take up at least 100 pixels to be considered valid [8]. The minimum blob size eliminates false alert rising from the environment noise but imposes a distance limitation. With regard to the blob size and the size of the drone, the longest distance between the drone and the camera was five meters. As shown in Figure 3**.** The moving object was detected by background subtraction and was denoted by the white pixels. The Kalman filter works as an adaptive filter, it uses the movement model to predict the movement path. If the moving object's path diverts from the predicted one, the Kalman filter corrects its movement parameter to fit the new path [9]. Figure 3 is a combination of all the frames, the white track shows the drone’s actual movement, and the red dot represents the center of the drone detected by the Kalman filter. The overall detected path was coherent with the actual movement, and it incorporated the drone’s acceleration even in constant velocity movement mode. There were several outliers in the middle of the path, but the offset was within the size of the drone. The Kalman filter requires the background to be stationary, thus the camera should be very stable. This poses challenges and raises the standards for the control mechanism. Despite that, the Kalman filter does not require manual training data input.

ArUco markers are used for mid range alignment estimation. When in midrange, the drone is likely to get out of the camera’s frame, thus reducing accuracy. The ArUco module is provided by OpenCV. Each ArUco code has its own unique identity and is stored in the system [10]. Figure 4 shows the same ArUco code with different orientations. Based on pattern distribution, the ArUco’s code roll, pitch and yaw were determined.

A square was used to replace ArUco code within MATLAB in an effort to integrate all software components. When the square faces the camera in parallel, the boundary is a square. Yaw, pitch, and roll distort the boundary from a square to a quadrilateral. With measured dimensions of the square and camera calibration, the distance between the square and camera can be determined.

Figure 3. Drone path tracking with a Kalman filter.

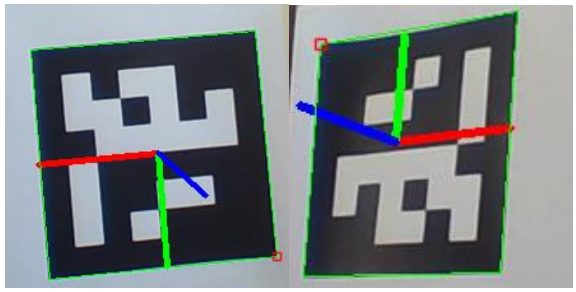

Figure 4. ArUCO Marker tracking for drone pose estimation.

4.1.4 Shell Design

The basic function of the shell is to host the magnets and sensors and to protect the drone during docking maneuvers and to accomplish all that with minimum weight. The shell was designed in Solid Edge which, given the material, can calculate the weight of the final object. The shell was 3D printed with ABS high impact, a light but strong polymer and one of the most used materials for 3D printing. To protect the drones during docking, the shell was designed with two sections stacked on top of each other as shown in Figure 5. The upper part which is located near the corners protects the propellers. The lower part in the middle provides support without blocking the camera view. From that decision onwards, every modification was to reduce the total weight. As an example, the skeletal patterns on the side were introduced to reduce the amount of material without compromising the strength. The final shell measured 350mm×350mm×40mm and weighed 107g.

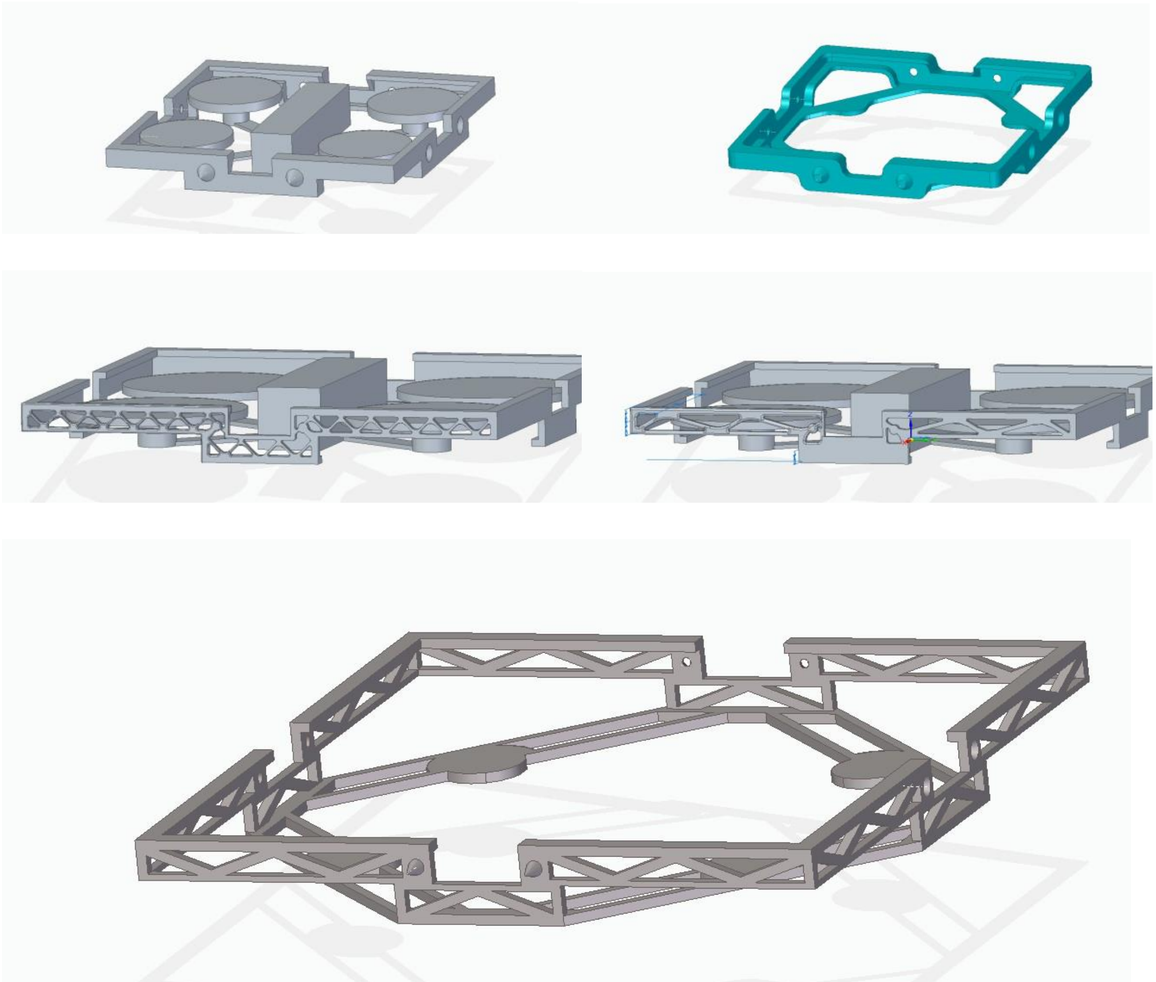

Figure 5. Evolution of the shell design

Due to its size, the shell was printed on four pieces and then glued with epoxy. This was not initially planned, and the design did not account for enough surface areas needed for gluing. Due to this unforeseen complication, glued joints became weak spots. Therefore, zip ties were used to provide more support.

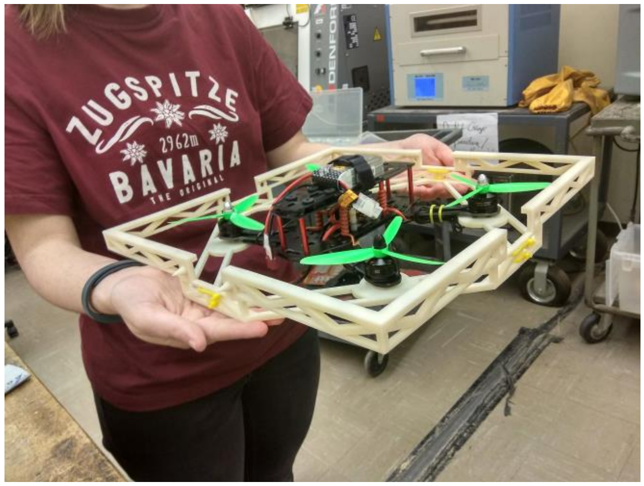

Figure 6. Printed shell attached to the drone.

4.1.5 Magnet Docking Mechanism

Electropermanent magnets were used to lock two neighboring drones together, enabling docking of the two vehicles. Two electropermanent magnets were mounted on each active side on a drone. The magnets were designed by the use of a pair of 25.4mm long, 4.62mm diameter cylindrical AlNiCo magnets [11], approximate 2035mm long 26 AWG coated copper wire, and a pair of washers constituting soft magnetic materials. The wire was wound tightly around one of the AlNiCo magnets. Then, two wire ends were crimped inside male terminals to assist with breadboard/PCB connection. The coiled AlNiCo magnet and bare one were held side by side between the two washers and then glued to the washers as shown in Figure 7. The assembled structure constitutes a single electropermanent magnet, referred to as magnet henceforth.

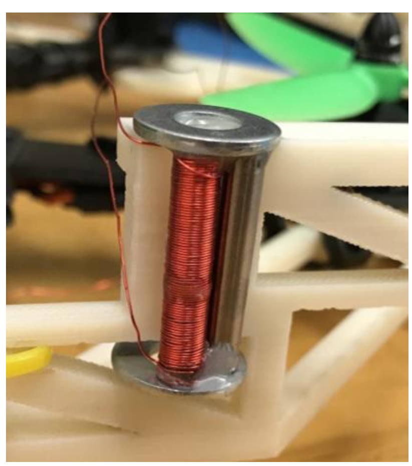

Figure 7. the assembled electropermanent magnet

Electropermanent magnets can be switched on or off via a short pulse of high current. When the electropermanent magnet is switched on, it attracts magnetic materials as shown in Figure 8. When the electropermanent magnet is switched off, it stops attracting magnetic materials.

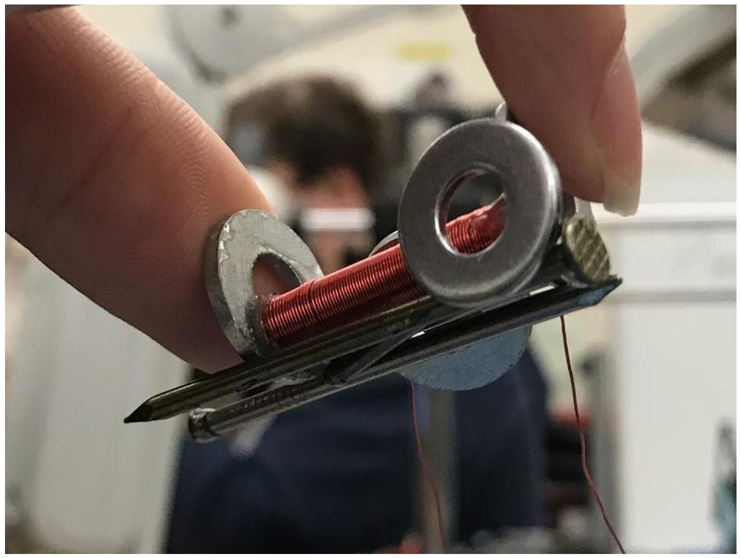

Figure 8. The electropermanent magnet when switched on attracts magnetic materials

The nature of electropermanent magnet switching lies in the ability to flip the polarity of AlNiCo magnets with a short pulse of current and the magnet's ability to maintain their new repolarized state. The amount of current needed to repolarize an AlNiCo magnet must generate enough magnetic field to overcome the magnetic coercivity of the AlNiCo magnets. For the specific magnets used in this project, the magnetic coercivity was 153kA/m [12].

The assembled electropermanent magnet was switched on or off with a short pulse of current. The current pulse traveling through the coil in one direction switches the magnet on while a current pulse traveling in the opposite direction switches it on. A boost converter was designed to collect a minimum of 50V of charge in a 47uF capacitor. The voltage build-up from 5V to 50V can be seen in Figure 9.

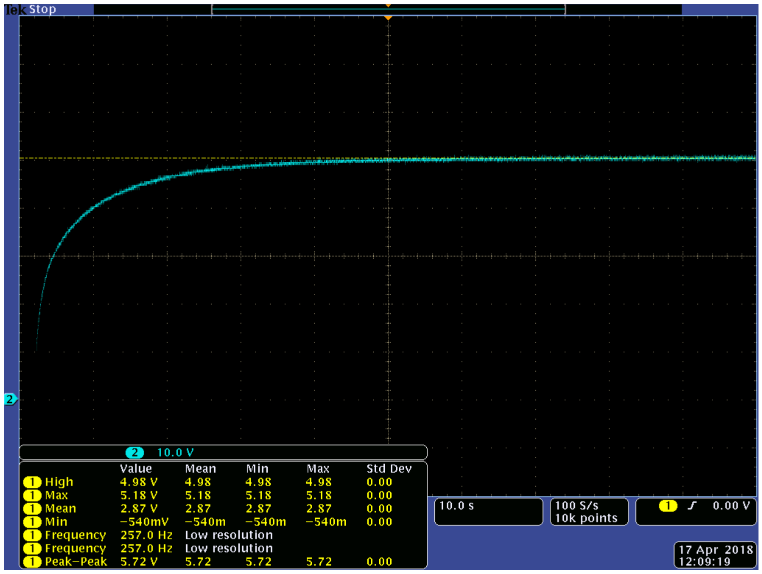

Figure 9. Charging a capacitor from 5V to 50V.

Capacitor charging was triggered by two different mechanisms, an RF signal from ground station and/or the short range alignment sensor system onboard the drone. Both activation methods were tested and worked successfully. Upon triggering, collected charge was then dissipated through the coil of wire wound around one of the AlNiCo magnets by manually flipping a switch. A MOSFET-controlled path for the current pulse, as shown in Figure 10. was investigated to automate the magnet switching process. However, the trials didn't prove successful as explained in the Constraints, Alternatives, and Tradeoffs section. Therefore, further testing and debugging are required for successful operation.

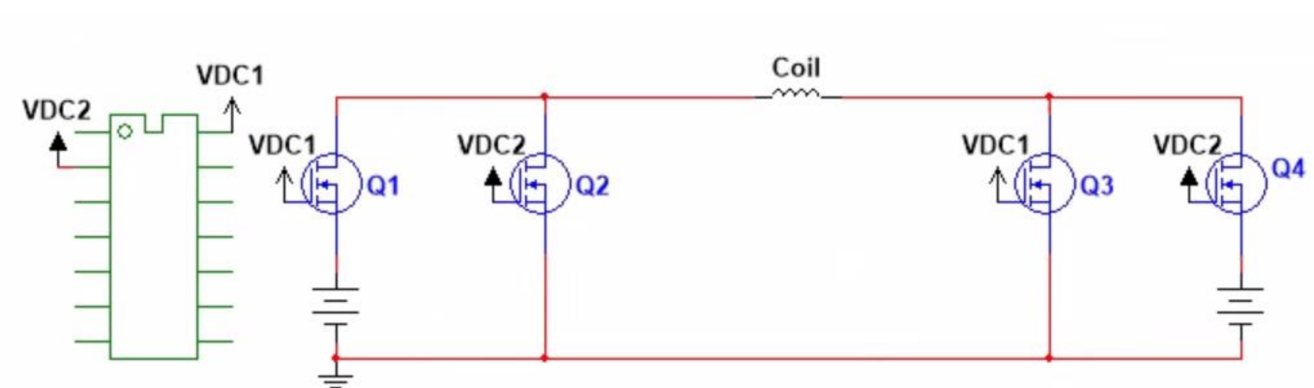

Figure 10. Controlling the current pulse path using MOSFET switches.

4.1.6 Control System

The control problem was divided into two main sections, stabilization and motor control. The general dynamics of a drone in the air compose of force in z direction and torques around three axes, as the four inputs to drive the system (1). To calculate the stabilization inputs, this drone model was linearized around the current state (2). This means adapting the working model on each loop according to the current position, orientation and velocities. This results in a drone model more accurate than the standard static linearization around an equilibrium point. This state space model enhanced precision, stability and disturbance rejection of the system.

$$\begin{pmatrix} \ddot{\vec{x}} \\ \ddot{\vec{\alpha}} \end{pmatrix} = \begin{pmatrix} mI_3 & 0 \\ 0 & I_{cr} \end{pmatrix}^{-1} \left(\begin{pmatrix} \vec{F} \\ \vec{M} \end{pmatrix} - \begin{pmatrix} 0 \\ \dot{\vec{\alpha}} \times I_{cr} \dot{\vec{\alpha}} \end{pmatrix} \right) \text{ rearranged } \dot{x} = f(x,u) \text{ where } x = \begin{pmatrix} \vec{x} \\ \vec{\alpha} \\ \dot{\vec{x}} \\ \dot{\vec{\alpha}} \end{pmatrix} \quad u = \begin{pmatrix} F_z \\ M_\alpha \\ M_\beta \\ M_\gamma \end{pmatrix} \tag{1}$$

$$\dot{x} = Ax + Bu \quad for \quad A = \left. \frac{\partial f(x,u)}{\partial x} \right|_{x=x_c, u=u_c} \quad and \quad B = \left. \frac{\partial f(x,u)}{\partial u} \right|_{x=x_c, u=u_c} \tag{2}$$

Cost matrices Q and R were used to evaluate importance of different states in stabilization. Q is the cost of the states, and R is the cost of the inputs. Minimizing the cost equation (3) derived a gain K that was implemented on the feedback loop for stability. This process is known as SDLQR or state dependant linear quadratic regulator. The outputs of the SDLQR are force and torque required for stabilization.

$$\min_u \int_0^\infty (x^T Q\, x \; + \; u^T R\, u)\, dt \quad s.t. \quad \begin{cases} u = -K\,x \\ K = R^{-1} B^T P \\ -A^T P - PA + PB\, R^{-1} B^T P - Q = 0 \end{cases} \tag{3}$$

$$Q\ is\ the\ cost\ of\ the\ states\ and\ R\ is\ the\ cost\ of\ inputs. Both\ symetric, semidefinte\ matrices$$

The calculated force and torques are passed to motor control. On a standard four propeller drone a square matrix relates this force and torques with the signal to be sent to the motors. However, this matrix becomes non-invertible for higher number of motors because the system has more variables than constraints. A nonlinear solver was implemented to solve the problem by minimizing the total power consumption by the motors, with the matrix equation as an equality constraint. The minimized cost function is a square norm of a vector; therefore, the system is guaranteed to find optimality (4).

$$\min_{u} \|\vec{u}\|^2 \quad s.t. \quad \begin{pmatrix} F \\ M_\alpha \\ M_\beta \\ M_\gamma \end{pmatrix} = \begin{pmatrix} k_F & k_F & \dots & k_F \\ L_{1,\alpha} \cdot k_F & L_{2,\alpha} \cdot k_F & \dots & L_{n,\alpha} \cdot k_F \\ L_{1,\beta} \cdot k_F & L_{2,\beta} \cdot k_F & \dots & L_{n,\beta} \cdot k_F \\ L_{1,\gamma} \cdot k_m & L_{2,\gamma} \cdot k_m & \dots & L_{n,\gamma} \cdot k_m \end{pmatrix} \begin{pmatrix} u_1 \\ u_2 \\ \vdots \\ u_n \end{pmatrix} \tag{4}$$

The matrix needed for this process encodes the dynamic properties of a given formation. Instead of manually calculating it the code on Appendix C derives such matrix from a user-friendly matrix that graphically show where the motors are located inside the formation and their rotation direction (5).

$$\begin{pmatrix} 0 & 0 & 0 & 0 & 0 & 0 & 0 & 0 \\ 0 & 0 & 0 & 0 & 0 & 0 & 0 & 0 \\ 0 & 0 & 0 & 0 & 0 & 0 & 0 & 0 \\ 0 & -1 & 1 & -1 & 1 & 0 & 0 & 0 \\ 0 & 1 & -1 & 1 & -1 & 0 & 0 & 0 \\ 0 & 0 & 0 & 0 & 0 & 0 & 0 & 0 \\ 0 & 0 & 0 & 0 & 0 & 0 & 0 & 0 \\ 0 & 0 & 0 & 0 & 0 & 0 & 0 & 0 \end{pmatrix} \Leftrightarrow \begin{pmatrix} 1.78 & 1.78 & 1.78 & 1.78 & 1.78 & 1.78 & 1.78 & 1.78 \\ 0.16 & 0.16 & 0.16 & 0.16 & -0.16 & -0.16 & -0.16 & -0.16 \\ 0.47 & 0.16 & -0.16 & -0.47 & 0.47 & 0.16 & -0.16 & -0.47 \\ -0.15 & 0.07 & -0.07 & 0.15 & 0.15 & -0.07 & 0.07 & -0.15 \end{pmatrix} \tag{5}$$

The entire system was implemented in a MATLAB function with the non-linear drone model for simulation. White noise was used to represent disturbance forces and torques on all axis. Magnetic interactions between drones were also modeled as disturbances. With the same controller, different drone formation were tested with step functions on x,y,z and yaw with a worst case scenario of 8.1% overshoot (See Figure 11).

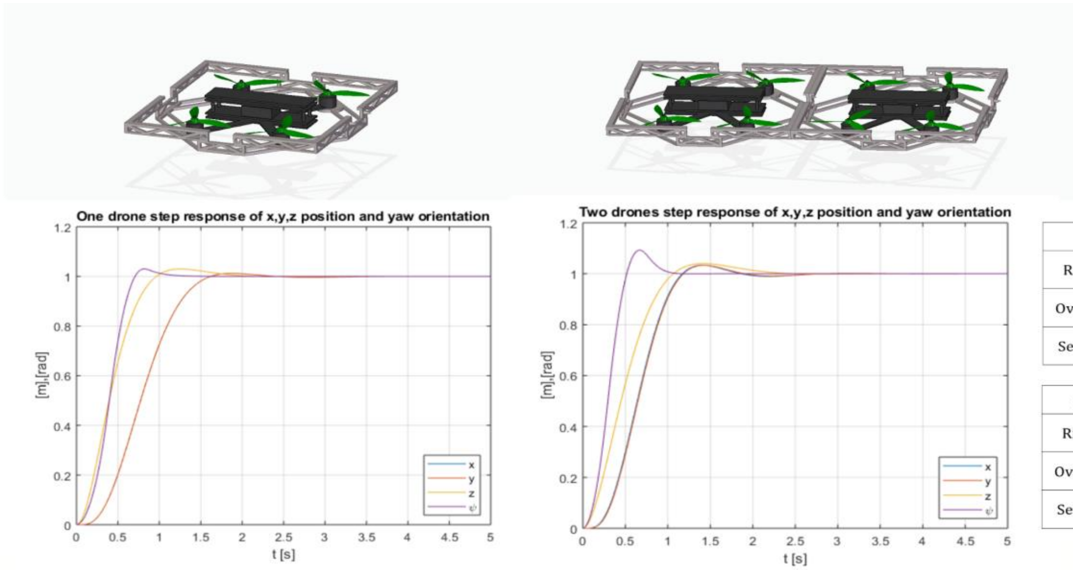

1 drone	x	y	z	Ψ
Rise time [s]	1.6	1.6	0.96	0.7
Overshoot [%]	1.2	1.2	3	3
Settle time [s]	2.4	2.4	2.2	1.5

2 drones	x	y	z	Ψ
Rise time [s]	1.2	1.2	1.1	0.52
Overshoot [%]	3.3	3.3	4	9.3
Settle time [s]	2.8	2.8	2.5	1.2

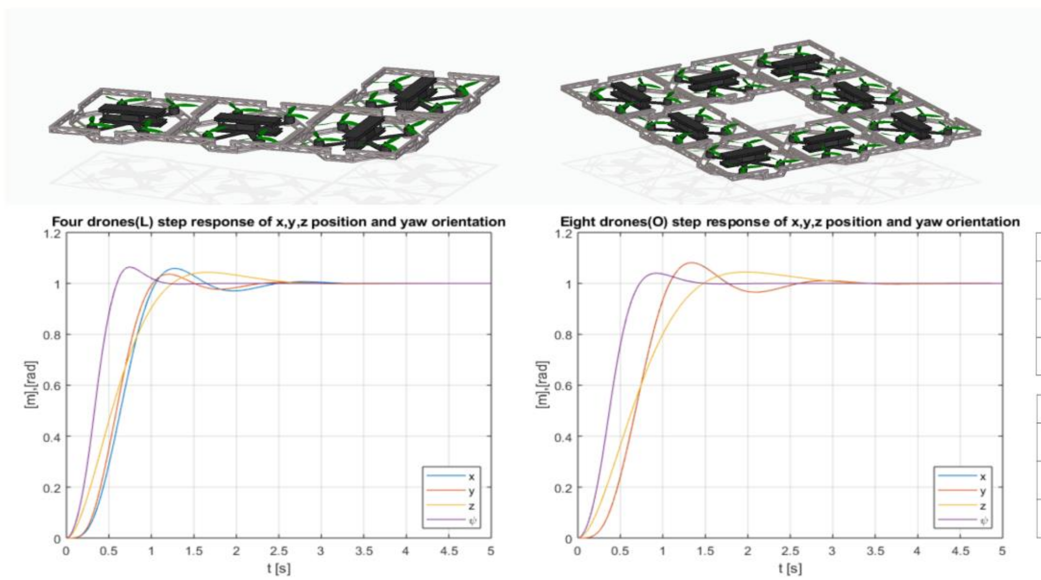

4 drones (L)	x	y	z	Ψ
Rise time [s]	1	1	1.2	0.6
Overshoot [%]	6	3.5	4.3	6.3
Settle time [s]	2.5	2.2	2.8	1.2

8 drones (O)	x	y	z	Ψ
Rise time [s]	1.1	1.1	1.5	0.73
Overshoot [%]	8.1	8.1	4.5	4
Settle time [s]	3.4	3.4	3.5	1.5

Figure 11. Step response comparison of four different drone formations.

Two drones successfully docked, flew together and undocked with disturbances in another simulation. (See Figure 12)

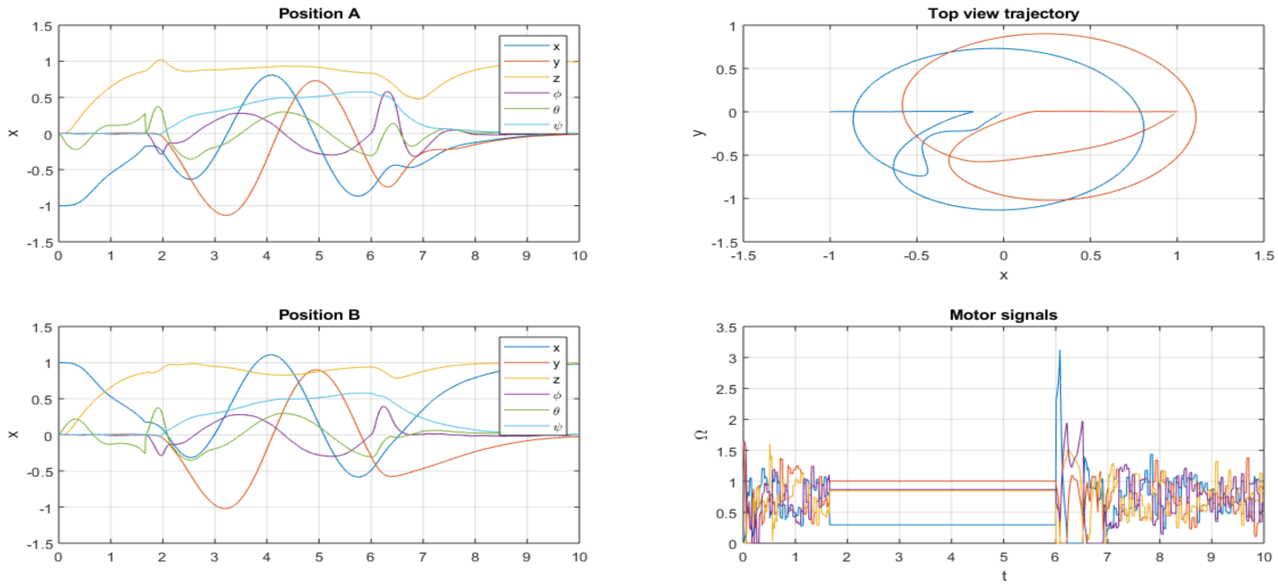

Figure 12. Docking maneuver, docked flight and undocking with disturbances.

Finally, a simulation was made with ever growing disturbances to compare the disturbance rejection of different drone formations. The result shows that disturbance rejection rapidly improves when the formation increases in size (See Figure 13). The best tested result comes from the eight drones formation, and its disturbance rejection performance is 100 times stronger than a signal drone. This is due to a combination of factors. First and foremost, the extra number of motors and the calculated optimal power distribution allow for stronger force and torque to counteract the disturbances without saturating the actuators. Secondly the larger weights and moments of inertia of the system reduce the influence of external forces and torques.

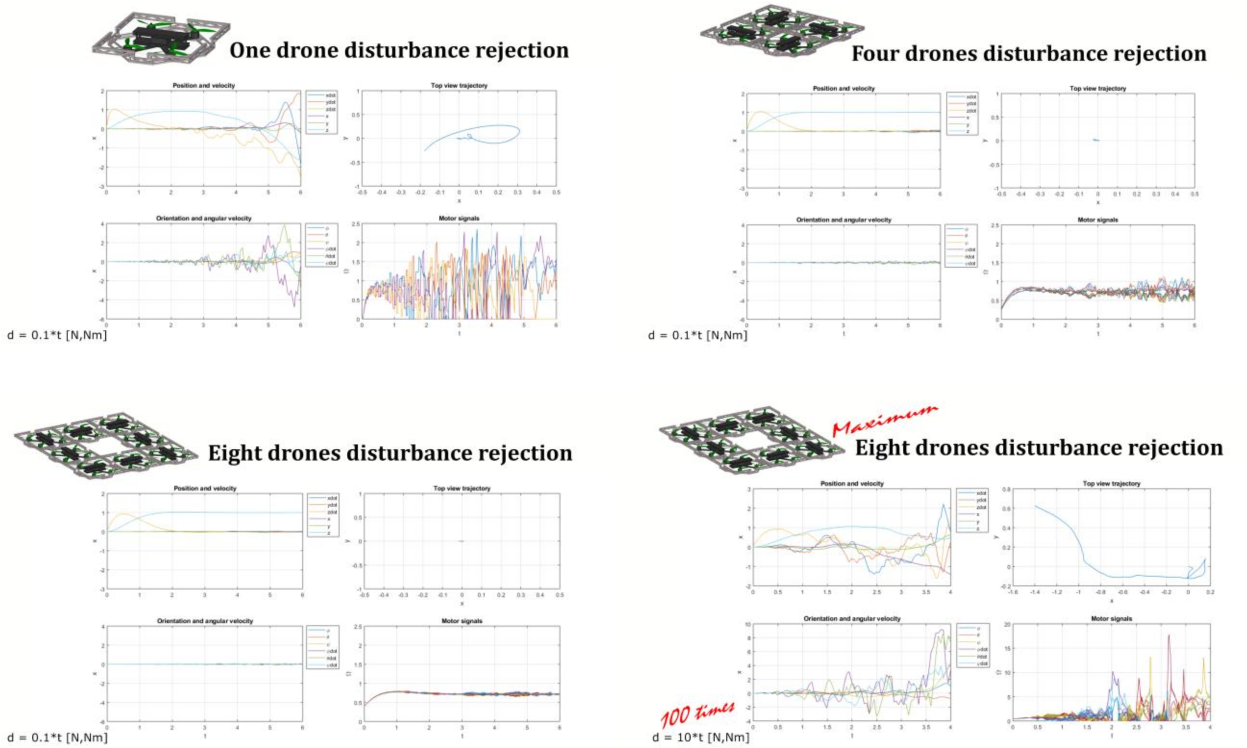

Figure 13. Disturbance rejection comparison.

For a better visualization, Simulink 3D animations were created alongside with the graphs (See Figure 14). The drone model is a parrot drone. However, all the dynamics parameters and the behaviors correspond to the SunFounder drone.

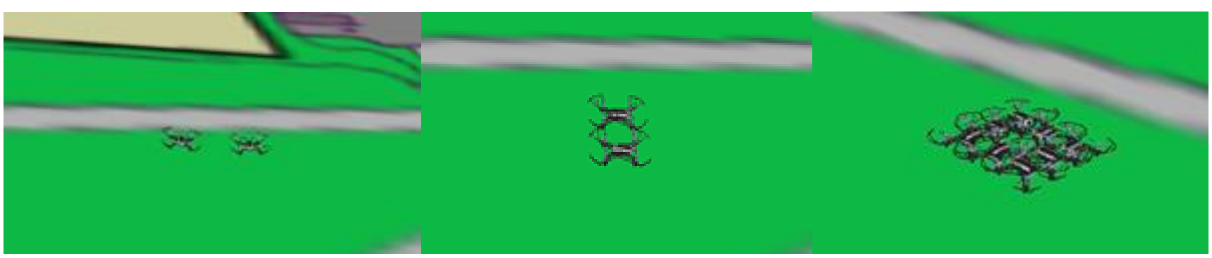

Figure 14. Simulink 3D animation of docking, docked flight and 8 drones formation flight.

4.1.7 Communication

Two different communication types were proposed for the successful operation of the project, drone-to-ground communication and drone-to-drone communication. Drone-to-ground communication took two different forms. One RF link was established between the drone with the electropermanent magnets and ground to trigger capacitor charging. For prototyping purposes, two nRF24L01 chips were connected to two different Arduinos. One Arduino had the magnet control circuit while the other had a trigger button. When the drones are within enough proximity to dock, the push button could be pressed to initiate the process of switching the magnet on. Another RF link was established between the remote controller and the drone to manually fly the drones by controlling the rotors. Drone-to-drone communication is yet to be implemented.

4.2 Codes and Standards

There were two most significant protocols that applied to this project. The first protocol is the Inter-Integrated Circuit (I2C) Protocol. This protocol was employed to allow multiple VL6180X and VL53L0X time-of-flight sensors to communicate with the microcontroller board, Arduino in our prototype case. The second protocol is S-BUS serial communication protocol. This protocol was developed by Futaba for motor control. S-Bus protocol was used as a link between the RF receiver on the drone and the remote controllers.

4.3 Constraints, Alternatives, and Tradeoffs

4.3.1 Drone

The original proposal indicated the use of Crazepony mini quadrotor. Further investigation of the drone showed that it may not support an increase in the payload. The drone itself weighs 46g. At the time of proposal, the added weight due to onboard sensors, magnets and soft magnetic materials was calculated around 47.95g. This weight does not include the weight of the shell, PCB or vector board and other extra parts. One option to alleviate the payload limitation issue is to find a more powerful battery and compatible motors. The investigated available motors that would fit the geometry of the Crazepony drone were not as powerful as the ones on the drone. SunFounder QAV250 drone was chosen as a replacement for the Crazepony drones. Despite having more than double the cost of the Crazepony drone, the SunFounder drones have more powerful batteries and motors and could support much higher payload without the flight time decreasing drastically. The cost change on the drone forced the project to have two drones instead of three. Unlike the Crazepony, the source code for the flight controller was not available for download online. Therefore, a BeagleBone board was considered as an alternative for the CC3D flight controller onboard the SunFounder drone.

4.3.2 Prototype general positioning

Positioning is one of the most complicated problems on any robotics project, even more on aerial projects. The most standard approach on controls research is to use a motion capture lab equipped with infrared cameras to have an accurate position feedback. Due to the focus of this project being on search and rescue and other outdoors applications, the decision was made to use onboard sensors and computation. This decision complicated the project but gave it a more solid selling point.

4.3.3 Shell material

The material choice for the shell had to be an equilibrium between weight and strength. On the field of aircraft models, styrofoam is the preferred material but it was a problem to create an equilibrated customized shell. On the other hand, 3D printing, the chosen option, had the advantage of accurate customized manufacturing and reduced infill density for the weight.

4.3.4 Automating Magnet Repolarization

The current design requires manually switching the current pulse path. Automatization of the process by the use of N-channel MOSFETs was investigated to minimize the user interaction with drones and improves the flexibility of the dynamic system by allowing drones to switch magnets on and off mid-flight without the intervention of ground station. Four Nexperia's BUK9832-55A/CUX N-channel MOSFETs were tested but no effect was observed on the magnet. The capacitor did discharge to approximately zero volts. Therefore, it was assumed that there was an alternative path for current to flow that wasn't through the coil. Another logical conclusion is that the MOSFETs add to the resistance of the discharge path and the energy is dissipated as heat rather than used for repolarization. However, the former conclusion seems to explain the lack of repolarization better because the added resistance to the MOSFET controlled path, 46 mΩ per transistor, is much less than the measured resistance of the coil, 1.2 Ω. Further investigation is needed to fully confirm this conclusion.

4.3.5 Close range positioning

The proposed method for close range positioning and alignment of drones was initially an infrared LED IR333-A and an infrared receiver TSOP38238. IR receiver readings can be impacted significantly depending on the ambient light or outdoor environments. Due to this limitation, laser rangefinders utilizing time-of-flight principles were adopted instead. Two types of laser rangefinders implemented in the project are VL53L0X and VL6180X. Using these time-of-flight sensors over LED system presented a tradeoff, due to the fact that the readings of these time-of-flight sensors are only single point measurements. These time-of-flight sensors are ideal for determining the distance of only the surface directly in front of it [7]. Thus, multiple readings might be needed to determine distance and to ensure accuracy. However, since the close range positioning was aimed at distances below 1 cm, single point measurements didn’t interfere with the consistency of the readings. A significant advantage gained by implementing laser rangefinders VL6180x is that compared to IR LED and IR receiver, they weigh considerably less [13].

4.3.6 Middle range positioning

Ultrasonic and computer vision can be both applied to positioning. For positioning the drones, in addition to distance information, orientation information is required. ArUco code is able to provide this information very effectively.

4.3.7 Long range positioning

Kalman Filter uses background subtraction method to detect moving objects, while machine learning relies on trained dataset. Kalman filter does not require massive amount of training data, and less than 30 frames of the beginning of the video is adequate for background detection. Its disadvantage is that it is only able to detect moving objects, regardless of the identity of the object. The other disadvantage is that the camera has to be stationary, and the process is very slow. On the other hand, machine learning and deep learning are more robust and are able to identify objects but requires a large set of training data. In the current stage of the project, Kalman filter was used mainly because of the lack of training data. Kalman filter was used based on the assumption that one drone stays stationary while the other drone flies towards it for docking.

4.3.8 Embedded Computing Solution

The ultimate goal for the SkyIsland prototype is to have all the components of the docking system and the flight controls system integrated under one powerful microcontroller. This would allow the docking mechanism to be unified with direct drone control under a unified software solution. The CC3D flight controllers initially installed with the SunFounder drones did not offer any software or hardware extensibility and lacked adequate computing power to govern both basic flight and execute high level programming. As a result, it deemed that the CC3D microcontroller, despite its relative simplicity and low power consumption, was inadequate in meeting the needs and demands of the SkyIsland system.

Instead, the BeagleBone Blue (BB Blue) and BeagleBone Black (BB Black) microcontrollers were considered as the unified computing solution of choice for SkyIsland. Ultimately, the BB Blue was the chosen computing solution for SkyIsland due to its integrated IMU/Barometer, WIFI/Bluetooth capabilities, and higher computing capacity over the BeagleBone Black (BB Black). Despite the hardware advantage of the BB Blue, the BB Black still offered a viable alternative through its extensively developed and established codebase. Due to the relatively recent launch of BB Blue in 2017, there is a lack codebase established for this hardware. The relative lack of software developed, configured, and compiled for the BB Blue platform meant a fair amount of software engineering outside the scope of the SkyIsland project. This shortcoming should become increasingly easy to overcome as the BB Blue hardware platform matures over time.

4.3.9 Software implementation

The original software solution was to run the ArduPilot software suite on the BB Blue and execute a large python program alongside the ArduPilot flight software in order to integrate the docking and flight functions. However, codebase issues with ArduPilot for the BB Blue prevented further development down this implementation. The second software implementation for the BB Blue involved utilizing the Robot Operating System (ROS). The issue with ROS, however, was that there was not a readily installable compilation and the entire codebase had to be built from source. After successfully building ROS on the BB Blue, the issue with ROS evolved to a lack of support for outside the lab drone operation from neither the available ROS applications. It is outside the scope of this project to develop a flight control solution from scratch either from the ROS API or otherwise.

With the lack of readily available drone software solutions, the final integration approach came to MATLAB and Simulink. The embedded coder from Simulink proved to be a powerful tool as basic I/O code blocks could be used in Simulink to control the BB Blue and streamlined the process for extensible programming. Additionally, drone localization and coupled-flight controls algorithms for the project were already implemented in MATLAB. Therefore, a Simulink integration solution is the most logical approach going forward for the continued development of SkyIsland.

5. Schedule, Tasks, and Milestones

Appendix A, lists all tasks and major milestones, team member(s) assigned to each specific task, and risk levels of these tasks. Appendix B contains a comprehensive Gantt chart presenting the timeline of the project.

6. Final Project Demonstration

The SkyIsland prototype consists of the following four functional modules and mechanisms for positioning, magnet repolarization control, communications, and control. The positioning module includes the Kalman filter and ArUco Code software as well as the time-of-flight sensors. RF transceivers and remote drone controllers are used for drone-to-drone and drone-to-ground communications. The magnet repolarization control circuit presently comes in two forms, a breadboard prototype and an improved PCB prototype. The control algorithm tracks a moving reference along the x, y, z, and yaw axes accounting for disturbances and magnetic influences. The control algorithm is still in the simulation phase with disturbances representative of realistic magnetic influences. The current progression of the project achieved successful implementation of aforementioned modules individually. However, integration of these modules into a single circuit and package was not achieved. The links to the videos referred below are in Appendix D.

- Close, mid, and long range positioning
    - Long range drone tracking was achieved with a Kalman filter and a demonstration can be seen in Figure 3. The trackable distance was measured to be around five meters.
    - Mid-range pose estimation was demonstrated in video 1 where the distance and orientations of a drone are detectable provided the ArUco code is entirely in the frame.
    - For close range detection, the distance limit was tested by comparing the distance measured from a ruler and the ToF sensor output measuring an object at the same position, and the results show the minimal operating distance is five millimeters. It is shown in video 2.

- Magnet repolarization and control circuit
  - The minimum magnetic field strength required for re-polarization was updated from 50 KA/m to 153 KA/m based on the AlNiCo magnet datasheet [12]
  - The power supply powering magnet repolarization comes from an Arduino and operates at 4.8 V. The magnet repolarization process was demonstrated in the following videos:
    - A digital multimeter (DMM) measures the capacitor's stored voltage which charges from 0 V to over 50 V, as shown in video 3.
    - A DPDT toggle switch is used to discharge the capacitor and direct the resulting current to repolarize the AlNiCo magnet, and the DMM displays the sudden drop of capacitor voltage.
    - The AlNiCo magnet holding nails and washers and following a pulse of re-polarizing current, drops the objects, as shown in video 4.
    - An unpolarized AlNiCo magnet without any magnetic force picking up washers and nails following a re-polarizing pulse of current, as shown in video 5.
  - To demonstrate the scalability of magnet system, a smaller PCB version of the magnet repolarization and control circuit was prototyped.
- Communication
  - Drone-to-ground communication was achieved through RF remote control, and the communication range is around 1000 m based on the transmitter and controller datasheet [14].
  - Drone-to-drone communication was achieved through a pair of nRF24L01 RF links.
    - The maximum communication range is 100 m based on the datasheet [15].
    - A pair of nRF24101 RF links was used during EXPO to demonstrate communications between two Arduinos, and this was shown in video 6.

- Bit rate and communication latency remain unmeasured for the RF link implementation.
- Eight commands are transmittable through the drone remote controller.

- Control System
    - The SkyIsland control system entails controlling multiple drones docked as a single unit to achieve stable flight as well as swarm operation of constituent drones maintaining stability during docking and undocking maneuvers.
    - Ground and Manual Control:
        - Two users can control the drones via remote control and maneuver them to a close vicinity of each other.
    - Matlab Simulations:
        - Single drone flight was simulated using both step functions and moving reference tracking with and without disturbances. Worst case scenarios returned a ±1.15º jitter for a drone subject to heavy disturbances.
        - A wide variety of formation flights were simulated with both step functions and moving reference tracking with and without disturbances. Worst case scenarios resulted in an 8.1% overshoot with eight drones in ring formation. Data from four examples of this simulation can be found in Figure 11.
        - Docking maneuvers, docked flight and undocking maneuvers were simulated with two drones subject to disturbances and changing magnetic interactions. An example of this simulation can be found in Figure 12.
        - Steady flight under growing disturbances with different formations were simulated. The time of destabilization for a constituent drone was used as the testing metric for all the different drone formations to compare their performance characteristics under the same set of disturbances. The results have

shown that an eight drone ring formation experienced approximately 100 times less fluctuation in position and 10 times less angle jittering under the tested disturbance conditions relative to a single drone. A final simulation was run to search for the maximum disturbance withstandable by the eight drones in ring formation, and results proved to be two orders of magnitude larger than the maximum disturbance withstandable by a single drone. Summaries of these simulations are shown in Figure 13.

  - Swarm:
    - Swarm behavior currently remains untested.
    - Constituent drones comprising the SkyIsland system remain on standby for a docking command from ground control. While they are not physically attached, their behavior and flight characteristics are influenced by the other drones in the swarm.

- Systems Integration
  - AlNiCo magnets were mounted on the active side of the shell on one prototype drone, and washers were mounted on the passive side of the shell on the other prototype drone.
  - A pair of time-of-flight (ToF) sensors were used to detect drone-drone distance and relative shell orientations. When the shell of the second drone is less than five centimeters away and its relative orientation is less than 10° from the first drone equipped with the ToF sensors, a signal will be sent to an LED to blink, as shown in video 7.
  - The capacitor charging process was triggered by a push button, and the capacitor's discharge was in turn triggered by a DPDT toggle switch.

- Operating time for the SkyIsland system was measured to last longer than eight minutes of flight time with both the shell and magnet assemblies mounted on the drones.

7. Marketing and Cost Analysis

7.1 Marketing Analysis

For search and rescue as well as aerial reconnaissance applications, there are currently no competing products on the drone market today which could mirror the aerial docking capabilities of the SkyIsland platform. However, two emerging autonomous drone platforms can compete against the capabilities of SkyIsland through sophisticated swarm software. Despite this, however, these competitors lack the flexibility, modularity, and on-mission hardware reconfigurability that SkyIsland provides [16, 17]. Current competing systems only offer swarm/fleet management and autonomous docking with a charging dock at a ground station [16, 17].

7.2 Cost Analysis

The team consists of five engineers working at an hourly rate of $45.00 part-time. Assuming a 6 hour weekly individual workload, the weekly personnel operating cost for the project comes out to be $1350.00 spanning over a period of 12 weeks for a total personnel cost of $16200.00 to develop the product. The drones can be reasonably acquired for $200.00 per unit, upgrading from the $90.00 unit cost of the prototype drones. The improved drones should comprise of a more power RF transmission and receiver system as well as an upgraded FPV gimbal camera system.

The SkyIsland system will be sold in kits of three individual drones which would put the material costs at $655.00 per kit. The cost of software development for the system is folded into the personnel cost as open-source tool sets will be utilized. In order to achieve reasonable market penetration, the SkyIsland kit will be priced at $2000.00 at launch. A total of 13 units of the kit will need to be sold in order recuperate the costs of R&D and materials.

TABLE 5
PROJECT LABOR BREAKDOWN AND ASSOCIATED COSTS.

Labor Type	**Salary (USD/Hr)**	**Weekly Hours**	**Total Cost (USD)**
Individual Work	$45 / Hour	4 Hours	$180.00
Group Work	$45 / Hour	2 Hours	$90.00
Total Work / Member	$45 / Hour	6 Hours	$270.00
Total Project Labor	**$225 / Hour**	**6 Hours**	**$1350.00**

TABLE 6
INDIVIDUAL SKYISLAND KIT COMPONENT COSTS.

Part Description	**Quantity**	**Unit Price (USD)**	**Total Cost (USD)**
SunFounder 250 Kit	2	$210.00	$420.00
Sparkfun ToF Sensors	4	$13.95	$27.90
BeagleBone Blue	2	$80.00	$160.00
AlNiCo Magnets	8	$3.75	$30.00
Backup Propellers	10	$1.70	$17.00

TABLE 7
PROJECTED TOTAL DEVELOPMENT COSTS.

Project Component	**Cost (USD)**
Labor	$16200.00
Prototype Materials & Parts	$655.00
Total	**$16855.00**

8. Conclusion

Presently, the team has demonstrated successful operation of project subparts where most of the specifications were met. Out of the three drones purchased, two drones were flown manually with and without a shell and stable flight was achieved. Manual docking of two drones was attempted multiple times without the help of alignment sensors. The drones were brought into close proximity of each other within the working range of sensors. Positioning sensors could have been used for aligning these drones and activating magnetic docking had the sensors been mounted on the drones. In addition, because the BeagleBone board was yet to be configured as a flight controller for the drones, automated docking could not have been attempted. The alignment sensors which are the dual ToF 2D alignment sensors and the 3D QR code alignment camera based sensor worked successfully when tested off-board. The docking magnets were designed and mounted on an active side of one drone and soft magnetic materials were mounted on the passive sides of the other drone during flight tests. The process of switching the magnets on or off was successfully triggered via two different approaches; an RF signal sent from the ground station and a triggering signal sent by a short range ToF sensor whenever the distance threshold is surpassed. However, the rest of the process needs further automatization and optimization via use of a software triggering current pulse path. Simulations of the control system were concluded successfully, and the control system could be implemented as a Matlab simulink executable on the BeagleBone board, but more localization sensors will be required for the successful operation of the control system. Currently, the drones lack spatial awareness since they are not currently equipped with an IMU, a GPS or camera assisted localization. Therefore, such sensors need to be added to solve the positioning problem. Generally, for the project to proceed to the next level, the current working sensors and docking magnets must be integrated and controlled by one BeagleBone board running the control system. One task that should be addressed in future work is connecting the motors to the new BeagleBone board and also maintains the current RF link with the remote controllers for ground station intervention and manual operation in case of emergencies. When all the current subsections are integrated, and flight tests are conducted, the number of drones in the swarm could be increased to more than two and an active communication network must be established. The team has already looked into possible standards and protocols for communications and the two most popular options are Wi-Fi and ZigBee. Although Wi-Fi is more commonly used, Zig-Bee seems to be a cheaper and more sustainable option since it seems to be more energy efficient. Once a network is set up, the drones in the swarm will be more capable of efficiently optimizing the use of the resources each drone has and the flight as one unit could be achieved.

One lesson the team has learned from working on this project is the importance of adapting to new situations and assigning tasks as early as possible. Another lesson is that integrating subsystems is not a step that should be left until all subsystems are perfected. It may be more sensible for subsystems to be put together as early in the project timeline as possible to speed the process of creating a working prototype. A final lesson the team has learned is to intelligently focus on the main problem and prioritize tasks accordingly. The goal of the project was to design a swarm of drone that can dock together. With this goal in mind, localizing the drones in space presented an important issue, and taking localization out of the equation would reduce the overall complexity of the project and would enable the team to focus on solving the actual problem of alignment and docking. Thus, narrowing down the main problem of the project and isolating extraneous factors became a very essential lesson to be learned in completing our project.

9. Leadership Roles

TABLE 8
LEADERSHIP ROLES OF THE TEAM

Leadership Role	Responsible Team Member	Responsibility Description
Budget and Purchase Coordinator	Ayca Ermis	- Keep a book of all team purchases - Submitting purchase forms on behalf of the Team
Documentation Coordinator	Ayca Ermis	- Keep an active thread of weekly reports
Expo Coordinator	Adrian de la Iglesia Valls	- Maintain all communication related to the expo and insuring team registration for the expo. - Relay expo related information to the rest of team
Graphic Designer	Adrian de la Iglesia Valls	- Produce 3D models, diagrams, and visual aids required for formal documents including but not limited to project proposal, poster and report
Securing Funding	Ayca Ermis	- Contact potential sponsors and ECE representatives
Sponsor Communication Coordinator	Lingfeng Zhou	- Arrange meetings for the team with the project sponsors

		- Maintain all communication related to sponsorship on behalf of the team
Supervisor Communication Coordinator	Jiaqing Li	- Communicate with the professor on behalf of the team - Keep the team informed of discussions with the professor
Video Editor	Latifah Almaghrabi Ayca Ermis	- Create a video documenting the work done on the project and showing a demonstration of the working prototypes - Create a teaser trailer for the project
Webmaster	Latifah Almaghrabi	- Ensure all the deliverables are accessible on the team's assigned website before due dates
Webmaster Assistant	Lingfeng Zhou	- Help the webmaster with web development issue as they arise - Develop an appropriate theme for the website
	Jiaqing Li	- Help the webmaster to compose any necessary write-ups for the website as instructed by the webmaster

10. References

[1] Kelsey D. Atherton. (2016, February), DroneBox is A Nest For Drones [Online]. Available: https://www.popsci.com/dronebox-is-nest-for-drones [Accessed 1 Dec. 2017].

[2] Daniel Briggs Wilson et al., “Guidance and Navigation for UAV Airborne Docking”, Robotics: Science and Systems, 2015.

[3] D. Rus, J. Romanishin, K. Gilpin, “Modular Angular-Momentum Driven Magnetically Connected Robots,” U. S. Patent 14, 067,132, 9 Oct., 2014.

[4] Peter Won et al., “Development of an Effective Docking System for Modular Mobile Self-Reconfigurable Robots Using Extended Kalman Filter and Particle Filter”, Robotics, vol. 4, pp. 25-59, 2015.

[5] Q. Quan, “Thrust and moments model on multicopters,” in Introduction to multicopter design and control, Springer, Singapore, 2017, pp-128.

[6] "Adafruit VL53L0X Time of Flight Distance Sensor - ~30 to 1000mm." Adafruit Industries, www.adafruit.com/product/3317.

[7]"Adafruit VL6180X Time of Flight Distance Ranging Sensor (VL6180)." Adafruit Industry, www.adafruit.com/product/3316.

[8]"Blob Analysis." Mathworks, www.mathworks.com/help/vision/ref/blobanalysis.html.

[9] "Using Kalman Filter for Object Tracking." MathWorks, www.mathworks.com/help/vision/examples/using-kalman-filter-for-object-tracking.html.

[10]"Detection of ArUco Markers." OpenCV,

docs.opencv.org/3.1.0/d5/dae/tutorial_aruco_detection.html.

[11]"Magnets and Actuators." Digi-Key Electronics, www.digikey.com/product-detail/en/littelfuse-inc/H-36-MAGNET/HE154-ND/475812.

[12] Littlefuse, “Magnets and Actuators,” H-36 datasheet, [Revised Nov. 2015].

[13] "SELECTING A SENSOR TECHNOLOGY." Acroname, acroname.com/blog/selecting-sensor-technology.

[14]Amazon. www.amazon.com/Crazepony-RadioLink-Transmitter-Receiver-Supporting/dp/B01FLWRY9Q.

[15]NORDIC SEMICONDUCTOR, “Single chip 2.4GHz Transceiver,” [Revised Mar. 2006].

[16] M. Murison, "Dronebox - The Automated, Connected, Self-Charging Drone Platform", Airnest: Simple Flight Planning & Analytics for Drones, 2017. [Online]. Available: http://www.airnest.com/blog/2016/2/18/dronebox-the-automated-connected-self-charging-drone-platform. [Accessed: Nov. 29, 2017]

[17] "Skysense", Skysense - Drone Charging Pad, 2017. [Online]. Available: http://www.skysense.co/. [Accessed: Nov. 29, 2017]

Appendix A: Task Distribution

Task Name	Task Lead[1]	Risk Level
Planning, Documentation and Presentations	**All**	**Low**
Research on drones	All	Low
Research on sensor parts	All	Low
Research on magnets	All	Low
Project Proposal	All	Low
Proposal Presentation (for parts)	All	Low
Ordering parts	All	Low
Final Project Presentation	All	Low
Final Project Demonstration	All	Medium
Final Project Report	All	Low
Demonstration video	LA, AE	Low
Docking Mechanism Design	**All**	**Medium**
Building magnet interlock	LA, AE	Low
Power electronics and circuit design	LA	Medium
Sensor-based alignment design	AE, JL	Medium
Ground Testing	All	Medium
Prototyping	**AIV, AE, JL,LA**	**Low**
Shell Assembly	AIV, AE	Low
Sensor Implementation	JL, AE	Low
Power electronics implementation	LA	Medium
Control Design and Implementation	**AIV**	**Medium**
Stability Control	AIV	Medium
Docking Control	AIV	High
Simulation Testing before implementation	AIV	Medium
Software Integration	**LZ**	**High**
Integration onto BeagleBone Black	LZ	High
Testing and Optimization	**All**	**High**
Indoor Testing	All	Medium
Field Testing	All	High

[1] AIV: Adrian de la Iglesia Valls, AE: Ayca Ermis, JL:Jiaqing Li, LA: Latifah Almaghrabi, LZ: Lingfeng Zhou.

Appendix B: Comprehensive Gantt Chart

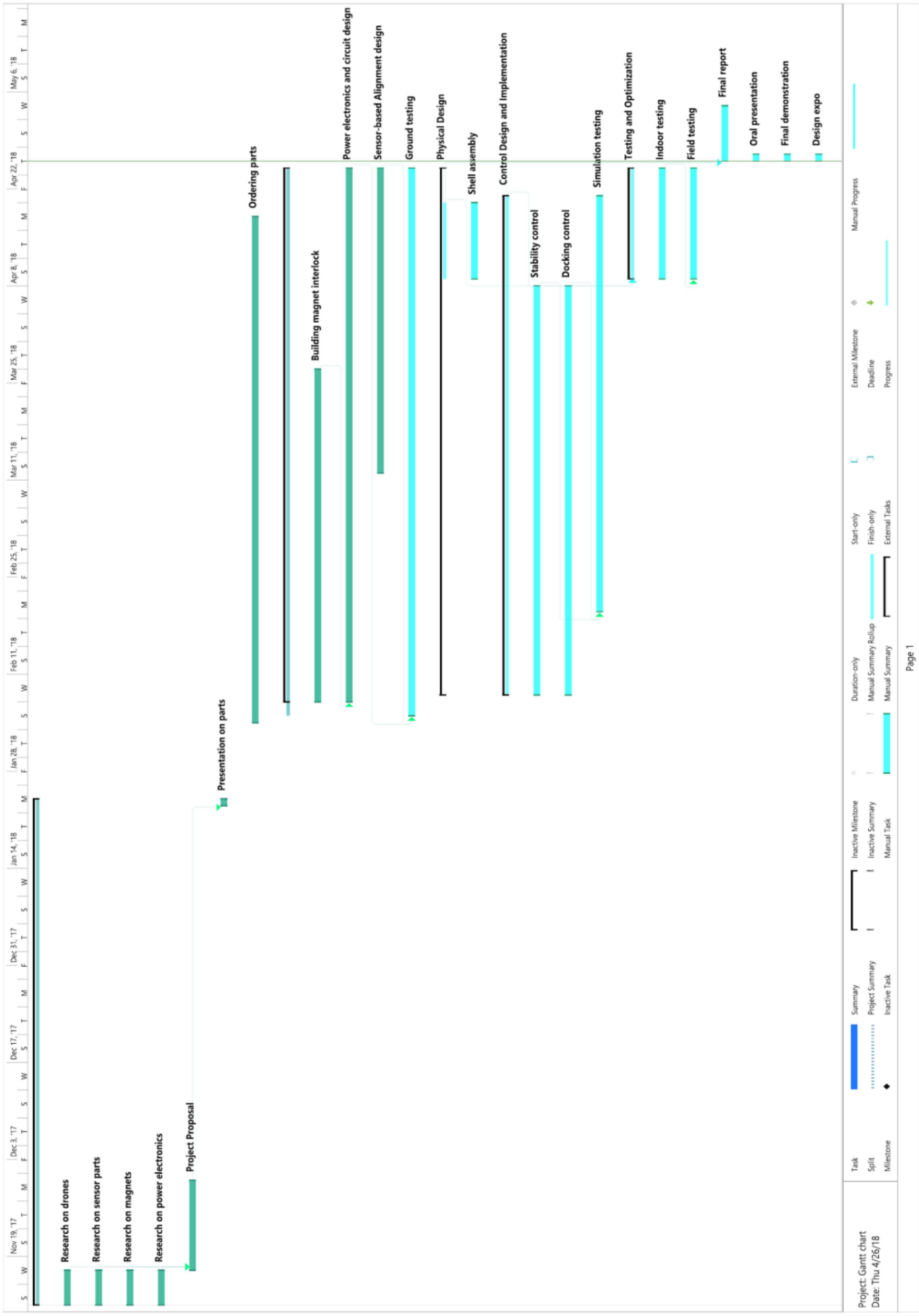

Appendix C: Matrix Calculation Code

```
C = [ 0  0  0  0  0  0  0  0  0;
      0  0  0  0  0  0  0  0  0;
      0  0  0  0  0  0  0  0  0;
      0  0  0  0  0  0  0  0  0;
     -1  1 -1  1  0  0  0  0  0;
      1 -1  1 -1  0  0  0  0  0;
      0  0  0  0  0  0  0  0  0;
      0  0  0  0  0  0  0  0  0];

L_u = 0.175;
m_u = 0.1298;
Ix_u = 0.0035;
Iy_u = 0.0036;
Iz_u = 0.0061;
kf = 1.78;
km = 0.53;

[M,Inertia] =  SetUp(C,L_u,m_u,Ix_u,Iy_u,Iz_u,kf,km);
-------------------------------------------------------------------------------

function [A,Inertia] =  SetUp(C,L,m_u,Ix_u,Iy_u,Iz_u,kf,km)
N_x=size(C)*[0;1];
N_y=size(C)*[1;0];
n=ones(1,N_y)*C.^2*ones(N_x,1);
x_cm=ones(1,N_y)*C.^2*[1:N_x]'/n;
y_cm=[N_y:-1:1]*C.^2*ones(N_x,1)/n;
m=n*m_u;
Ix=n*Ix_u;
Iy=n*Iy_u;
Iz=n*Iz_u;
L_x=[];
L_y=[];
L_z=[];
p=1;
while p<=n
 for k=1:N_y
  for j=1:N_x
    if C(k,j)~= 0
     x(p)=j;
     y(p)=N_y-k+1;
     spin(p)=C(k,j);
     L_x=[L_x,(y(p)-y_cm)*L];
     L_y=[L_y,-(x(p)-x_cm)*L];
     L_z=[L_z,spin(p)*sqrt((y(p)-y_cm)^2+(x(p)-x_cm)^2)*L];
     Ix=Ix+m_u*((y(p)-y_cm)*L)^2;
     Iy=Iy+m_u*((x(p)-x_cm)*L)^2;
     Iz=Iz+m_u*((y(p)-y_cm)^2+(x(p)-x_cm)^2)*L^2;
     p=p+1;
    end
  end
 end
end
a_1=kf*ones(1,n);
a_2=kf*L_x;
a_3=kf*L_y;
a_4=km*L_z;
A = [a_1;a_2;a_3;a_4];
Inertia = [m,Ix,Iy,Iz];
end
```

Appendix D: Video Repository

Video 1

https://drive.google.com/open?id=1-X-87CBY9iCq7R0v-DZyLNeT7XtklVqU

Video 2

https://drive.google.com/open?id=1DW5IRLiZyjqWIYqJOHFsSKfq3cgsNoOv

Video 3

https://drive.google.com/open?id=1at-Yh6qaAqzs5wem8Ytft8E7XT1yLo6-

Video 4

https://drive.google.com/open?id=12BzbQJhe9J5QSY3WYbfZl8oibiLsc4Z3

Video 5

https://drive.google.com/open?id=10Nz6Rw02mHlc2Sb2f5_jl4k70NrdACd9

Video 6

https://drive.google.com/open?id=1_wfYGGa1mNgScKEt5C4QqMDKNN-NrQfy

Video 7

https://drive.google.com/open?id=1_wfYGGa1mNgScKEt5C4QqMDKNN-NrQfy